The Astrophysical Journal, 780:84 (8pp), 2014 January 1 doi:10.1088/0004-637X/780/1/84

BINARY–DISK INTERACTION. II. GAP-OPENING CRITERIA FOR UNEQUAL-MASS BINARIES

Luciano del Valle and Andrés Escala
Departamento de Astronomía, Universidad de Chile, Casilla 36-D, Santiago, Chile; ldelvalleb@gmail.com
Received 2013 May 8; accepted 2013 October 1; published 2013 December 13

ABSTRACT

We study the interaction of an unequal-mass binary with an isothermal circumbinary disk, motivated by the theoretical and observational evidence that after a major merger of gas-rich galaxies, a massive gaseous disk with a supermassive black hole binary will be formed in the nuclear region. We focus on the gravitational torques that the binary exerts on the disk and how these torques can drive the formation of a gap in the disk. This exchange of angular momentum between the binary and the disk is mainly driven by the gravitational interaction between the binary and a strong nonaxisymmetric density perturbation that is produced in the disk, in response to the presence of the binary. Using smoothed particle hydrodynamics numerical simulations, we test two gap-opening criteria, one that assumes the geometry of the density perturbation is an ellipsoid/thick spiral and another that assumes a flat spiral geometry for the density perturbation. We find that the flat spiral gap-opening criterion successfully predicts which simulations will have a gap in the disk and which will not. We also study the limiting cases predicted by the gap-opening criteria. Since the viscosity in our simulations is considerably smaller than the expected value in the nuclear regions of gas-rich merging galaxies, we conclude that in such environments the formation of a circumbinary gap is unlikely.

Key words: binaries: general – black hole physics – galaxies: nuclei – hydrodynamics – methods: numerical

Online-only material: color figures

1. INTRODUCTION

A binary embedded in a gaseous disk is a configuration that is repeatedly found in astrophysics at a variety of scales. Some examples are the interaction between planetary rings and satellites (Goldreich & Tremaine 1982), the formation of planets in protoplanetary disks and their migration (Goldreich & Tremaine 1980; Ward 1997; Armitage & Rice 2005; Baruteau & Masset 2013), the evolution of stellar binaries (Shu et al. 1987; McKee & Ostriker 2007), the interaction of stars and black holes in active galactic nuclei (Goodman & Tan 2004; Miralda-Escude & Kollmeier 2005; Levin 2007), and the expected interaction of massive black hole (MBH) binaries at the center of merging galaxies. In all these cases, it is fundamental to have a proper understanding of the main dynamical processes that drive the evolution of a binary–disk system.

MBH binaries that interact with gaseous disks are expected to form in the context of hierarchical structure formation (White & Frenk 1991; Springel 2005). In this scenario, the formation and evolution of galaxies is a complex process, in which their final states will be sculpted by a sequence of mergers and accretion events. If the galaxies involved in these mergers are rich in gas, there is theoretical (Barnes & Hernquist 1992, 1996; Mihos & Hernquist 1996; Barnes 2002; Mayer et al. 2007, 2010) and observational (Sanders & Mirabel 1996; Downes & Solomon 1998) evidence that a large amount of the gas will reach the central kiloparsec of the newly formed system. Also, there is observational evidence for the existence of an MBH at the center of practically all observed galaxies with a significant bulge (Richstone et al. 1998; Magorrian et al. 1998; Gultekin et al. 2009). Therefore, it is expected that the MBH in the center of each galaxy follows the gas flow to form a MBH binary embedded in a gas environment in the central parsec of the newly formed galaxy, as seen in a variety of numerical simulations (Kazantzidis et al. 2005; Mayer et al. 2007; Hopkins & Quataert 2010; Bournaud et al. 2011).

Although numerical simulations suggest the formation of MBH binaries, the only conclusive evidence of pairs of black holes comes from the observation of quasar pairs with separations of ∼100 kpc (Hennawi et al. 2006; Myers et al. 2007, 2008; Foreman et al. 2009; Shen et al. 2011; Liu et al. 2011) and some accreting black holes with separations on the order of or smaller than 1 kpc (Komossa et al. 2003; Fabbiano et al. 2011; Comerford et al. 2012). On the other hand, there is evidence of at least one MBH binary with a separation of a few parsecs (Rodriguez et al. 2006), but in general, observational evidence for bound MBH binaries remains elusive, and most candidates have observational signatures that can be explained by other configurations and processes different from a MBH binary (Valtonen et al. 2008; Komossa et al. 2008; Boroson & Lauer 2009; Tsalmantza et al. 2011; Eracleous et al. 2011; Dotti et al. 2012; references therein).

Considering the lack of observational evidence, it is crucial to obtain more insight into the dynamical process of binary–disk interaction, to determine in what type of merger remnants it is more probable to find these binaries and how the binary separation of these systems depends on the characteristics of the central parsec of the merger remnants.

A considerable amount of work and progress on understanding the interaction of a MBH binary with a gas environment has been made since Escala et al. (2004, 2005) showed, with numerical simulations, that "when the binary arrives at separations comparable to the gravitational influence radius of the black hole ($R_{\rm inf} = 2GM_{\rm BH}/(v^2 + c_{\rm s}^2)$)," (Escala et al. 2005, p. 158) the binary stars locally dominate the total gravitational field and the gas tends to follow the gravitational potential of the binary, forming a nonaxisymmetric density perturbation that interacts gravitationally with the binary and drives a decrease of the binary separation. Because of the self-similar nature of the gravitational potential, the nonaxisymmetric density perturbation is also self-similar in nature in the regime where the gravitational potential is dominated by the MBH binary. This suggests that although in

the simulations of Escala et al. (2004, 2005) the shrinking of the binary stops at the gravitational resolution, the fast decay will continue down to scales where the gravitational wave emission is effective enough to bring the binary to coalescence.

For systems such as those explored by Escala et al. (2004, 2005), where the gas mass of the disk is much greater than the binary mass, it is expected that the time the binary takes to merge will be on the order of a few initial orbital times (Escala et al. 2005; Dotti et al. 2006), unless a dramatic change happens in the nearby gas of the binary where the strong nonaxisymmetric density perturbation forms (such as gap formation or gas ejection by the black hole accretion luminosity). This contrasts with the results of simulations of disks with masses that are negligible compared with the binary mass, where the coalescence time is found to be several thousands of local orbital times (Artymowicz & Lubow 1994; Ivanov et al. 1999; Armitage & Natarajan 2002; Milosavljević & Phinney 2005), which for $M_{\rm BH} \geqslant 10^7\,M_{\odot}$ is even longer than the Hubble time (Cuadra et al. 2009).

This fast–slow (a few orbital times versus several thousand) migration duality can also be found in simulations of protoplanetary disks that harbor planets (e.g., extreme mass ratios; Ward & Hourigan 1989; Ward 1997; Bate et al. 2003; Armitage & Rice 2005; Baruteau & Masset 2013; Kocsis et al. 2012a, 2012b). In this type of simulation, the planet–star binary is an extreme mass ratio binary ($q \ll 1$) and the fast and slow migration regimes are defined as type I and type II migration. In the type I regime, the protoplanetary disk experiences a perturbation due to the small gravitational potential of the planet. This allows a fast migration of the planet (on the order of a few $t_{\rm orb}$) with a characteristic timescale that scales as the inverse of the planet mass ($t_{\rm migration} \propto M_{\rm p}^{-1}$). Type II (slow) migration is experienced by a planet when its Hill radius is greater than the local pressure scale height of the protoplanetary disk ($R_{\rm Hill} \gg h$). In this case, the disk perturbation due to the presence of the planet becomes important, and the planet begins to excavate a gap in the disk. This leads to coupled evolution of the planet and the disk on a viscous timescale, making the migration time much longer.

For the case of a comparable-mass binary embedded in a disk, as in the extreme mass ratio case of a star–planet–disk system, the threshold between fast and slow migration is also determined by the formation of a gap or cavity in the disk. Therefore, if we can determine for which systems a gap will be opened, we can determine in which systems a fast or slow migration will occur. For this reason, in a previous work (del Valle & Escala 2012; hereafter Paper I) we derived a gap-opening criterion that we tested with numerical simulations of equal-mass binaries embedded in gas disks. We found that the gap-opening criterion, and hence the threshold between the fast and slow regimes, is determined by the relative strength between the gravitational and viscous torques. In this paper, our aim is to extend the study of gap-opening criteria to the case of binaries with moderate mass ratio ($0.1 \leqslant q \leqslant 1$).

This paper is organized as follows: In Section 2, we extend the analytic gap-opening criterion derived in Paper I to the case of moderate mass ratio binaries ($0.1 \leqslant q \leqslant 1$). In Section 3, we present the setup of the numerical simulations that we use to test the extended analytic gap-opening criterion. In Section 4, we describe how we identified the formation of a gap in our numerical simulations, and we test the extended analytic gap-opening criterion against the simulations. In Section 5, we study why the formation of a gap in some simulations is not well predicted by the extended gap-opening criterion and derive a new gap-opening criterion that is consistent with all our numerical simulations. In Section 6, we study the limits for the final evolution of a binary embedded in a gas disk that are predicted by this successful analytic gap-opening criterion. Finally, in Section 7 we discuss the implication of our results for real astrophysical systems and present our conclusions.

2. GAP-OPENING CRITERIA FOR UNEQUAL-MASS BINARIES

The most widely studied case of binary–disk interaction is that of a binary embedded in a gas disk with much smaller mass than the mass of the primary. This limiting case of a low-mass disk ($M_{\rm disk}/M_{\rm primary} \ll 1$) is typically found in the late stages of star or planet formation (Lin & Papaloizou 1979; Goldreich & Tremaine 1982; Takeuchi et al. 1996; Armitage & Rice 2005; Baruteau & Masset 2013). In these studies, when the binary has an extreme mass ratio ($q \ll 1$), the gravitational potential produced by the secondary is treated as a perturbation to the axisymmetric gravitational potential of the primary–disk system, allowing a linear approximation for the equations of motion of the secondary. From this approximation, studies have found that the sum of the torques arising from the inner and outer Lindblad and corotation resonances drive the interaction between the secondary and the disk. This approach leads to predictions of gap structure that are consistent with simulations within the same regime of validity ($q \ll 1$ and $M_{\rm disk}/M_{\rm primary} \ll 1$) (Ivanov et al. 1999; Armitage & Natarajan 2002; Nelson & Papaloizou 2003; Haiman et al. 2009; Baruteau & Masset 2013).

Motivated by the success of this approach in the planetary regime ($q \ll 1$), some authors have extrapolated this analysis to other cases where $q \sim 1$ (Artymowicz & Lubow 1994, 1996; Gunther & Kley 2002; MacFadyen & Milosavljević 2008) regardless of the strong nonlinear perturbation that is produced by the nonaxisymmetric gravitational field of the binary, which breaks the validity of the linearization of the equation of motion in this regime ($q \sim 1$; Shi et al. 2012).

In this paper, we study the case of binaries with moderate mass ratio ($0.1 \leqslant q \leqslant 1$) interacting with a gaseous disk of comparable mass ($M_{\rm disk}/M_{\rm bin} \sim 1$) without any assumption of linearity. We consider the tidal nature of the binary–disk interaction to model the torques between the binary and the disk instead of a resonant process such as the one that appears in the linear approximation. This tidal torque approach is motivated by the work of Escala et al. (2004, 2005), where it was found that the exchange of angular momentum between an equal-mass binary and a disk is driven by the gravitational interaction between a strong nonaxisymmetric density perturbation on the disk and the equal-mass binary. Using this approach, Paper I successfully tested an analytical criterion for the formation of a gap in the case $q = 1$, assuming that the gravitational interaction between this strong nonaxisymmetric density perturbation and the binary was the main process driving the exchange of angular momentum between the disk and the binary. We extend our gap-opening criterion to the case of binaries of unequal but comparable mass ($0.1 \leqslant q \leqslant 1$), for which the nonaxisymmetric potential of the binary is still sufficiently strong to drive the formation of a strong global nonaxisymmetric density perturbation in the disk.

The shape and size of the strong nonaxisymmetric density perturbation is determined by the dominant gravitational potential of the binary, whose typical scale length is the binary separation. Therefore, as in Paper I, we can assume that the torque produced by the nonaxisymmetric density perturbation on the

binary can be written as $\tau = -a^2 \mu \rho G K_q$, where ρ is the density of the perturbation, a is the binary separation, which determines the scale length of the nonaxisymmetric density perturbation, $\mu = m_1 m_2/(m_1 + m_2)$ is the reduced mass of the binary, and K_q is a parameter that depends on the geometry of the density perturbation. In principle, K_q can depend on the mass ratio of the binary, because the shape of the nonaxisymmetric density perturbation is determined by the nonaxisymmetric gravitational potential of the binary.

To derive the criterion for the opening of a gap in the disk, we follow the same procedure used in Paper I. We compare the gap-opening timescale $\Delta t_{\rm open}$ (determined by the torque that the binary exchanges over the disk) with the gap-closing timescale $\Delta t_{\rm close}$ (Goldreich & Tremaine 1980). Gap formation requires that $\Delta t_{\rm open} < \Delta t_{\rm close}$, and therefore it is straightforward to find that the binary will open a gap in the disk if

$$\frac{\Delta t_{\rm open}}{\Delta t_{\rm close}} = \frac{1}{f_{\rm q}} \left(\frac{c_{\rm s}}{v}\right)^3 \left(\frac{v}{v_{\rm bin}}\right)^2 \leqslant 1\,, \qquad (1)$$

where $f_{\rm q} = 2K_q/\alpha_{\rm ss}$ with $\alpha_{\rm ss}$ being the dimensionless viscosity parameter of Shakura & Sunyaev (1973), v the rotational speed of the binary–density perturbation system, $v_{\rm bin}$ the Keplerian velocity of the binary, and $c_{\rm s}$ the sound speed of the gas in the disk. In this form, the gap-opening criterion depends on the relative strength between the gravitational and viscous torques ($K_{\rm q}/\alpha_{\rm ss}$), the thermal and rotational support of the disk ($c_{\rm s}/v$), and the relative strength between the total mass of the system and the mass of the binary ($v/v_{\rm bin}$).

3. INITIAL CONDITIONS AND NUMERICAL METHOD

We ran smoothed particle hydrodynamics (SPH) simulations to study the binary–disk interaction and test the generalization of our gap-opening criterion. All our simulations consist of a coplanar unequal-mass binary of mass ratio q, initial separation a_0, and mass $M_{\rm bin}$ embedded in an isothermal and stable ($Q > 1$) gas disk of radius $R_{\rm disk}$ and mass $M_{\rm disk}$. In these simulations, we use a natural system of units where [mass] = 1, [distance] = 1, and $G = 1$. In these units, we set the initial radius of the disk as $R_{\rm disk} = 30$ and the mass of the disk as $M_{\rm disk} = 30$ for all the runs. The disk of gas is initialized with the same density profile that we used in Paper I: a constant surface density for $R < R_{\rm c}$ and $\propto R^{-1}$ for $R > R_{\rm c}$, where $R_{\rm c} = 0.1\,R_{\rm disk} = 3$, and a vertical density profile that has the functional form $\cosh(z/H_{\rm d})$, where $H_{\rm d}$ is constant for $R < R_{\rm c}$ and $\propto R$ for $R > R_{\rm c}$. With this setup, the mass of the disk in the inner region ($R < R_{\rm c}$) is $M_{\rm gas}(<R_{\rm c}) = 1$.

The parameter space that we explore with our numerical simulations is determined by the variation of four parameters, a_0, $M_{\rm bin}$, $h_{\rm c}$, and q, in the ranges $a_0 \in [2, 6]$, $M_{\rm bin} \in [1, 33]$, $h_{\rm c} \in [0.8, 3]$, and $q \in [0.1, 1]$. We ran 16 simulations (see Table 1) with different combinations of these parameters.

Following the numerical setup used in Paper I, we include a fixed Plummer potential (Plummer 1911) with a total mass $\sim 0.12\,M_{\rm disk}$. This external potential helps stabilize the disk and will mimic the existence of an external stellar component when we apply our result to the study of supermassive black hole (SMBH) binaries.

The gaseous disk is modeled as a collection of 5×10^5 SPH particles with gravitational softening of 0.1. This resolution is 2.5 times greater that used in Paper I. In Appendix B of Paper I, we proved that our conclusions are the same for simulations with 2×10^5 SPH particles and 1×10^6 SPH particles. Therefore, the number of particles that we use to model the disk in this paper is large enough to numerically test the gap-opening criterion. For the binary, we use two collisionless particles with gravitational softening of 0.1.

Table 1
Run Parameters

RUN	q	$a_0/R_{\rm disk}$	$M(<r)/M_{\rm bin}$	$(c_{\rm s}/v_{\rm bin})^2$	$Q_{\rm min}$
A1	0.1	0.100	0.0125	3.110	2.62
A2	0.1	0.133	0.0222	1.780	2.20
A3	0.1	0.133	0.0133	2.220	2.20
A4	0.1	0.200	0.0500	4.650	2.19
B1	0.3	0.100	0.0125	1.037	2.62
B2	0.3	0.133	0.0222	0.593	2.20
B3	0.3	0.133	0.0133	0.740	2.20
B4	0.3	0.200	0.0500	1.550	2.19
C1	0.5	0.100	0.0125	0.622	2.62
C2	0.5	0.133	0.0222	0.365	2.20
C3	0.5	0.133	0.0133	0.444	2.20
C4	0.5	0.200	0.0500	0.930	2.19
D1	1.0	0.100	0.0125	0.311	2.62
D2	1.0	0.133	0.0222	0.178	2.20
D3	1.0	0.133	0.0133	0.222	2.20
D4	1.0	0.200	0.0500	0.465	2.19

In all simulations, the disks are stable. In Table 1, we specify the minimum value of the Toomre parameter Q for each simulation. At the beginning of all our simulations, the gravitational potential of the binary–disk–Plummer system has a nonnegligible nonaxisymmetric component due to the contribution of the binary. Therefore, the disk lacks a well-defined velocity profile $v_\phi(r)$. For this reason, we calculate the initial rotational velocity of the system using the same procedure as in Paper I. A symmetric representation of the gravitational potential of the binary is used to compute the initial velocity of the gas. We use the initial orbital radius of the secondary as the radius of this symmetric representation. We refer the reader to Appendix A of Paper I for more details of this implementation.

4. STUDYING THE GAP-OPENING CRITERION FOR UNEQUAL-MASS BINARIES

To test the analytic gap-opening criterion against the SPH numerical simulations described in the previous section, we first need to define what a gap is. For this purpose, we use the same numerical criterion as in Paper I (see Section 2 for details) to determine in which of our simulations the binary opens a gap in the disk. We will only outline the key aspects of this numerical criterion.

To determine if a gap is formed in a certain time t, we seek two characteristics: (1) a density peak in the perimeter of the gap, whose maximum has to be greater than 0.015 (in internal units of the code), and (2) that the semimajor axis a of the binary does not decrease by more than 10%. With these two characteristics, we define a numerical threshold to determine in which simulations a gap is formed. We define disks with a gap as all those where conditions 1 and 2 are fulfilled, and disks without a gap as all those where neither condition 1 nor 2 is fulfilled. We refer to every simulation where a gap is formed as an opened simulation and every simulation where there is no gap as a closed simulation. The times at which we analyze our simulations are the times in which the binary completes 2, 3, 5, 7, 10, and 15 orbits. For more details on these conditions and their justification as traits of gap formation, we refer the reader to Section 2 of Paper I.

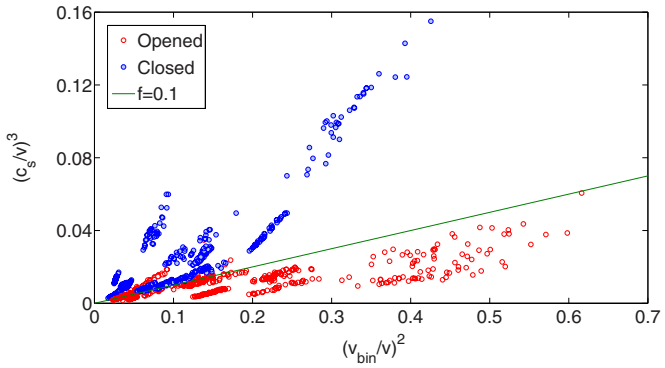

Figure 1. Cubic ratio between the sound speed of the gas and the rotational velocity of the binary–disk system, $(c_s/v)^3$, plotted against the quadratic ratio between the rotational velocity of the isolated binary and the rotational velocity of the binary–disk system, $(v_{bin}/v)^2$. The red circles indicate simulations where the binary has opened a gap in the disk (opened simulations), and the blue circles are simulations where the disk does not have a gap (closed simulations). We plot together all the simulations with different values of the mass ratio q that we explore. The straight line is the linear q-independent threshold between the opened simulations and the closed simulations predicted by our analytic gap-opening criterion. Below the line are the opened simulations and above are the closed simulations. The slope of the interface is the function f.

(A color version of this figure is available in the online journal.)

In Figure 1, we plot the opened (open circles) and closed (filled circles) simulations. In this plot, the horizontal axis is $(v_{bin}/v)^2$ and the vertical axis is $(c_s/v)^3$. Each point corresponds to a given time at which we analyzed a simulation. We use the secondary's orbital speed as the speed of the binary–density perturbation system (v) because the strong nonaxisymmetric density perturbation is formed by the gas that tends to follow the gravitational potential of the binary and therefore corotates with it.

It can be seen from Figure 1 that the groups of opened and closed simulations populate two different regions of parameter space. The region that is populated by the opened simulations is the region for which the opening time of a gap is shorter than the closing time ($\Delta t_{open} < \Delta t_{close}$), and the region populated by the closed simulations is the region for which the closing time of a gap is shorter than the opening time ($\Delta t_{open} > \Delta t_{close}$). Therefore, the threshold between these two regions is where the gap-closing time is equal to the gap-opening time. We can find the expected shape of this interface by evaluating our gap-opening criterion [Equation (1)] for the limiting case $\Delta t_{open} = \Delta t_{close}$. For this limit, in the parameter space $((v_{bin}/v)^2, (c_s/v)^3)$, the gap-opening criterion predicts that the interface between these two set of simulations has a linear shape with slope $m_q = f_q = 2\,K_q\,/\,\alpha_{ss}$.

We first explore whether the linear threshold can be assumed to be q-independent (i.e., $m_q = f$), even though the geometry of the density perturbation (K_q) is expected to be q-dependent. This assumption implies that in Figure 1 a line of slope f will be sufficient to model the threshold between the opened and closed simulations. We find that the slope of this line is $m = f = 0.1$.

Figure 1 shows that although this line separates fairly well the distributions of closed and opened simulations, there are some simulations (17% of the total number) that are inconsistent with this threshold line. This discrepancy is even greater for the simulations with mass ratio $q = 0.1$, 40% of which have positions in parameter space that cannot be explained by this q-independent threshold line. This suggests that the value of f_q cannot be assumed to be q-independent.

In Figure 2, we test whether a q-dependent slope for the threshold line is a better assumption. We separate the simulations into four different plots for different values of q. In each, the axes are the same as in Figure 1 and we use a different slope $m_q = f_q$ for the threshold line. The q-dependent thresholds increase the number of simulations that are consistent with the gap-opening criterion, in comparison with the q-independent line: we find that the values of the q-dependent slopes that better separate the closed simulations from the opened ones are $f_{q=1} = 0.098$, $f_{q=0.5} = 0.100$, $f_{q=0.3} = 0.110$, and $f_{q=0.1} = 0.180$.

For the case $q = 1$ [Figure 2(a)], we find that all the simulations are well separated by this q-dependent linear threshold, in agreement with our previous results (Paper I). For the other mass ratios, the q-dependent linear thresholds separate almost all our simulations well, but there are still some simulations that are not consistent with the threshold lines. These deviations are most important for the simulation with mass ratio $q = 0.1$ [Figure 2(d)], but even for this extreme case, fewer than 10% of the simulations deviate from the prediction of our q-dependent gap-opening criterion. In the next section, we explore possible causes for these deviations.

5. DEVIATIONS AND THEIR CAUSES

In the previous section, we tested the analytic gap-opening criterion and found that, despite its simplicity, it successfully predicted the distribution of opened and closed simulations in most cases. However, some simulations, at certain times, have positions in the space of parameters (Figure 2) that are inconsistent with this criterion. For example, for $q = 0.3$ and $q = 0.1$ [Figures 2(c) and (d), respectively], it is clear that a linear threshold is not the best curve to explain the separation of closed and opened simulations, even if the slopes are not the same for all the values of q that we explore. In order to explain these deviations, we focus on the approximations that we used to derive this gap-opening criterion.

In Section 2, for the derivation of our analytic gap-opening criterion we restricted the geometry of the nonaxisymmetric density perturbation to an ellipsoid with a scale length equal to the binary separation a. For this geometry, the gravitational torque produced on the binary by the density perturbation has a quadratic dependence on the binary separation and can be expressed as $\tau = a^2 G \mu K_q$.

The assumption of an ellipsoidal geometry is based on the work of Escala et al. (2004, 2005), where it was found that for the majority of the numerical simulations, the response of the gas to the gravitational potential of a binary has an ellipsoidal shape. However, the numerical simulations of Escala et al. (2004, 2005) in which the formation of such ellipsoidal density perturbations is present are far from the regime where a gap can be formed.

In our numerical simulations, we explored the parameter space in the vicinity of the gap-forming regime, and we find that the density perturbation has a spiral shape instead of an ellipsoidal one (Figure 3). Such spiral-shaped density perturbations were also found by Escala et al. (2005) in two of their simulations (Figures 10 and 12), which are in the same gap-forming regime as our simulations.

The torque produced on the binary by such spiral-shaped density perturbation will have the same quadratic dependence on the binary separation a only if the vertical scale of the spiral is comparable to its radial scale (the thick-spiral limit). Therefore, the torque given by $\tau \propto a^2$ that we used in the derivation of our analytic gap-opening criterion will be valid only for the cases where the spiral density perturbation is in the thick-spiral limit.

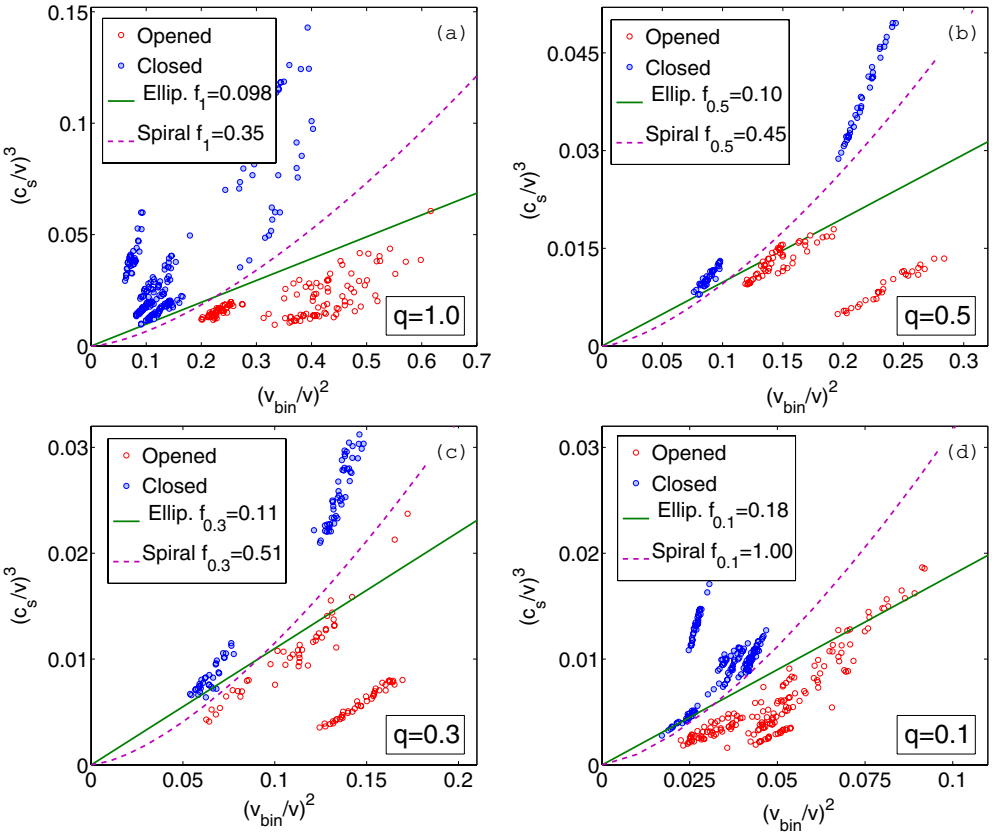

Figure 2. Same as Figure 1, but with q-dependent thresholds for our ellipsoidal gap-opening criterion. The dashed curves are the threshold between the opened simulations and the closed simulations predicted by our flat spiral gap-opening criterion (see Section 5). For all panels, the flat spiral gap-opening criterion successfully separates the closed simulations from the opened simulations. In (a), for the equal-mass binaries ($q = 1$) both the flat spiral gap-opening criterion and the ellipsoidal gap-opening criterion successfully separate the closed from the opened simulations.

(A color version of this figure is available in the online journal.)

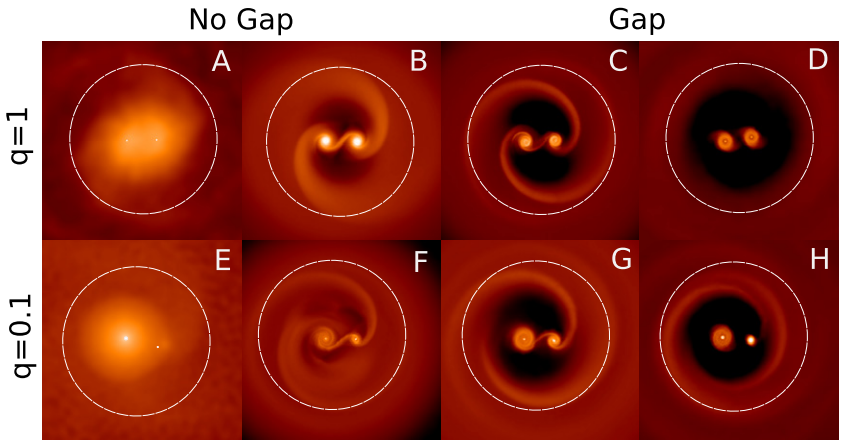

Figure 3. Surface densities from eight simulations for two different values of q. The white circles enclose the region $r < 2a$ of the disk, with a the binary separation. From left to right, the panels show a binary far from the gap-forming regime, a binary with parameters in the vicinity of the gap-forming regime that does not form a gap in the disk, a binary that begins to excavate a gap on the disk, and a binary that excavates a gap in the disk. The geometry of the density perturbation is spiral for the simulations within the gap-forming regime ((c), (d), (g), and (h)) and for the simulation in the vicinity of the gap-forming regime ((b) and (f)). In contrast, we can see that for the simulation that is far from the gap-forming regime, the density perturbation has an ellipsoidal geometry for $q = 1$ and a pear shape for $q = 0.1$ [(a) and (e)].

(A color version of this figure is available in the online journal.)

The spiral density perturbations that are formed in our simulations tend to be more flat than thick, and therefore the thick-spiral limit may not be valid for all simulations. For a flat spiral, the radial scale length of the perturbation is determined by the binary separation a, and as the flat spiral pattern is embedded in the disk, its vertical scale height is truncated by the thickness of the disk ($h_{\rm spiral} \sim H_{\rm disk}$). Therefore, the torque produced by this flat spiral density perturbation can be written as $\tau_s = a H_{\rm disk} G \mu K_q$, where the product $a H_{\rm disk}$ is associated with the flat spiral geometry.

From the torque produced by a flat spiral geometry, we derive a new gap-opening criterion following the same procedure as in

Section 2:

$$\frac{\Delta t_{\rm open}}{\Delta t_{\rm close}} = \frac{1}{f_{\rm q}} \left(\frac{c_{\rm s}}{v}\right) \left(\frac{v}{v_{\rm bin}}\right)^2 \left(\frac{H_{\rm disk}}{a}\right) \leqslant 1\,. \quad (2)$$

To test whether the assumption of a flat spiral geometry for the density perturbation is a better approximation for our simulations, we compare the shape of the threshold between the group of closed and opened simulations predicted by Equation (2) in the limit $\Delta t_{\rm open} = \Delta t_{\rm close}$ with the shape of the threshold predicted by the ellipsoidal criterion [Equation (1) in the limit $\Delta t_{\rm open} = \Delta t_{\rm close}$].

Assuming for simplicity that $H_{\rm disk}/a = c_{\rm s}/v$, we compare the flat spiral gap-opening criterion with the ellipsoidal criterion in the parameter space $((v_{\rm bin}/v)^2\,,\ (c_{\rm s}/v)^3)$. In Figure 2, the dashed lines represent the q-dependent thresholds between the closed and opened simulations predicted by the flat spiral criterion. For this criterion, the values of the q-dependent parameter $f_{\rm q}$ that better describe the threshold between the closed and the opened simulations are $f_{q=1} = 0.35$, $f_{q=0.5} = 0.45$, $f_{q=0.3} = 0.51$, and $f_{q=0.1} = 1.00$.

This threshold has a shape that better separates the closed from the opened simulations, compared with the linear threshold predicted by the ellipsoidal gap-opening criterion. In fact, all the simulations that are not consistent with the linear threshold are consistent with the flat spiral gap-opening criterion.

For the case of equal-mass binaries [Figure 2(a)], the thresholds predicted by the flat spiral and ellipsoidal gap-opening criteria separate the closed and opened simulations equally well. In this case, the parameters of the systems that we explore are in the vicinity of the regime $a \sim H_{\rm disk}$, where the torque associated with the flat spiral geometry ($\tau \propto a H_{\rm disk}$) and the torque associated with the ellipsoidal geometry ($\tau \propto a^2$) have comparable values, making them indistinguishable. On the other hand, in our simulations, the unequal-mass binaries [Figures 2(b)–(d)] are in systems where the thickness of the disk tends to be smaller than the binary separation, and therefore the ellipsoidal torque and the flat spiral torque have different values.

6. LIMITS FOR FINAL BINARY EVOLUTION

The nonaxisymmetric density perturbation that is formed in the disk by the presence of the binary is self-similar in nature, and hence when the binary shrinks, the nonaxisymmetric density perturbation also shrinks. Therefore, the gravitational interaction between the binary and the nonaxisymmetric density perturbation will continue to reduce the binary separation unless there is a dramatic change in the nearby gas, such as the formation of a gap.

From the flat spiral gap-opening criterion, we can evaluate how likely it is that this decrease of binary separation will lead, or not, to the formation of a gap. This is particularly important in the context of the evolution of SMBH binaries, where the formation of a gap may stop the shrinking of the binary at separations where the emission of gravitational waves is not efficient enough to drive the final coalescence of the SMBH.

Assuming for simplicity a disk with a Mestel (1963) density profile, we can write our flat spiral gap-opening criterion [Equation (2)] with an explicit dependence on the binary separation a as

$$\left(\frac{c_{\rm s}^2 H_{\rm disk}}{G M_{\rm bin}}\right) \left(\frac{H_{\rm disk}}{q\,a} + \frac{H_{\rm disk}}{R_{\rm disk}} \frac{M_{\rm disk}}{M_{\rm bin}}\right) \leqslant \left(\frac{K_{\rm q}}{\alpha_{\rm ss}}\right)^2, \quad (3)$$

where we used the relations $r_2 = (1+q)^{-1} a$, $\mu = q M_{\rm bin}/(1+q)^2$, $v_{\rm bin}^2 = G\mu/a$, $v^2 = G((M_{\rm gas}(r_2)/r_2) + v_{\rm bin}^2(a/r_2))$, and, for a Mestel disk, $M_{\rm gas}(r_2) = r_2\, M_{\rm disk}/R_{\rm disk}$.

From Equation (3), it can be seen that the flat spiral gap-opening criterion is a decreasing function of a if the disk thickness $H_{\rm disk}$ is constant or does not depend strongly on a. In this case, the decrease of the binary separation will not drive the system toward the formation of a gap. In fact, the decrease in separation will drive the binary away from the regime where it is possible to form a gap.

Although the assumption of a flat spiral geometry for the density perturbation is more accurate for modeling the transition from closed to opened simulations, the density perturbation on systems where $a \ll H_{\rm disk}$ is expected to have an ellipsoidal geometry instead of flat spiral geometry (this can be seen, e.g., in the simulations of Escala et al. 2004, 2005). For this reason, we also studied the ellipsoidal gap-opening criterion. Using the same relations that we used to derive the Equation (3), we can write the ellipsoidal gap-opening criterion [Equation (1)] with an explicit dependence on a as

$$\left(\frac{c_{\rm s}^2 H_{\rm disk}}{G M_{\rm bin}}\right) \left(\frac{1}{q}\left(\frac{H_{\rm disk}}{a}\right)^3 + \frac{H_{\rm disk}^3}{a^2\, R_{\rm disk}} \frac{M_{\rm disk}}{M_{\rm bin}}\right) \leqslant \left(\frac{K_{\rm q}}{\alpha_{\rm ss}}\right)^2 \quad (4)$$

One can see from Equation (4) that the ellipsoidal gap-opening criterion (like the flat-gap opening criterion) is a decreasing function of a if the disk thickness is constant or does not depend strongly on a. Therefore, the decrease in binary separation will not drive the system toward the formation of a gap.

In Equations (3) and (4), we assumed that the disk has a Mestel density profile, for which the enclosed mass has the form $M_{\rm gas}(r) = M_{\rm disk}(r/R_{\rm disk})$. If we assume that the disk has a steeper density profile, the enclosed mass will be a less steep, or even decreasing, function of r. Accordingly, Equations (3) and (4) will be more strongly decreasing functions of a. Hence, although the assumption of a Mestel density profile for the disk is not based on any expected condition of the density profile in real systems, the results and conclusions derived assuming such a profile are also valid for any other steeper profile.

It is important to note that when $a \ll H_{\rm disk}$ we can assume that the disk thickness does not depend on the binary separation, because at scales much greater than the binary separation, the binary gravitational potential looks like the gravitational potential of a single object of mass $M_{\rm bin}$. Moreover, the thickness of the disk will be determined by the total mass of the binary and disk and the thermal state of the disk. Therefore, we can conclude that for systems where a gap has never formed, the decrease of binary separation to the limiting case $a \ll H_{\rm disk}$ will not lead to the formation of a gap.

From this analysis, we can conclude that in a large variety of systems a gap will never be opened/formed unless some other process (other than the formation of a gap due to the binary–density perturbation gravitational interaction) changes the distribution of the nearby gas. This supports the idea that it is likely that the gas will drive the shrinking of the separation of SMBH binaries down to scales where gravitational wave emission is efficient enough to allow their subsequent coalescence.

7. DISCUSSION AND CONCLUSIONS

In simulations of comparable-mass binaries ($q \sim 1$) embedded in gas disks, studies have found that the timescale for the shrinking of the binary separation can be on the order of a few orbital times (the fast migration regime; e.g., Escala et al. 2004, 2005; Dotti et al. 2006) or a few thousand orbital times (the slow migration regime; e.g., Artymowicz & Lubow 1994; Ivanov et al. 1999; Armitage & Natarajan 2002; Milosavljević & Phinney 2005; Cuadra et al. 2009). The threshold between the fast and slow migration regimes for comparable-mass binaries, as in the planet migration case (extreme mass ratio binaries, $q \ll 1$), is determined by the formation of a gap in the disk. Therefore, in this work, we tested a gap-opening criterion that would enable us to estimate in what systems fast or slow migration will proceed.

For the case of equal-mass binaries, Escala et al. (2004, 2005) found that the exchange of angular momentum between the binary and a gaseous disk is driven by the gravitational interaction between the binary and a strong nonaxisymmetric density perturbation with an ellipsoidal geometry. Considering this gravitational interaction, in a previous publication (Paper I) we derived a gap-opening criterion that we tested numerically for equal-mass binaries. In the present work, we studied whether this ellipsoidal gap-opening criterion is also valid for binaries with moderate mass ratio ($0.1 \leqslant q < 1$). For this purpose, we ran 12 SPH simulations of binaries with moderate mass ratio embedded in gas disks and tested the validity of the analytic ellipsoidal gap-opening criterion against the simulations.

We find that the analytic ellipsoidal gap-opening criterion [Equation (1)] successfully predicts that the simulations where a gap is formed (opened simulations) and the simulations where there is no gap in the disk (closed simulations) are distributed into two separate regions in $((v_{\rm bin}/v)^2$ v/s $(c_{\rm s}/v)^3)$ parameter space (see Figure 1).

However, there are some simulations, at certain times, with positions in this parameter space that are inconsistent with the ellipsoidal gap-opening criterion (see Figure 2). These deviations are most important for the case of binaries with mass ratio $q = 0.1$, where roughly 9% of the total number of these simulations, at certain times, are inconsistent with the ellipsoidal gap-opening criterion.

In our simulations, we find that the strong nonaxisymmetric density perturbation has a flat spiral geometry rather than the ellipsoidal geometry that we used to derive the ellipsoidal gap-opening criterion (see Figure 3). Therefore, we have derived a new gap-opening criterion using a flat spiral geometry for the density perturbation. We find that this flat spiral gap-opening criterion [Equation (2)] is q-dependent and successfully separates the closed from the opened simulations. In fact, all the simulations that we explored are consistent with this flat spiral gap-opening criterion (see Figure 2), including the roughly 9% of simulations with mass ratio $q = 0.1$ that were inconsistent with the ellipsoidal gap-opening criterion.

The difference between the geometry of the density perturbation that we found in our simulations and the geometry found in the simulations of Escala et al. (2004, 2005) is the result of the different regimes that these simulations explored. In our simulations, we explore the vicinity of the gap-forming regime, while the simulations of Escala et al. (2004, 2005) are in general far from the gap-forming regime.

Far from the gap-forming regime, the gravitational torque that the binary produces on the disk is efficiently absorbed and dissipated through the disk ($\Delta t_{\rm close} \ll \Delta t_{\rm open}$). Therefore, the gas corotates with the binary in a quasi-equilibrium configuration, and its structure follows the geometry of the gravitational equipotential of the binary, which for $q = 1$ has an ellipsoidal shape. On the other hand, our simulations have parameters in the vicinity of the gap-forming regime ($\Delta t_{\rm open} \sim \Delta t_{\rm close}$), for which the angular momentum deposited in the gas through the gravitational torque exerted by the binary is not efficiently dissipated through the disk, producing a radial flow of gas. In this nonequilibrium state, the density perturbation takes a spiral shape, like that observed in our simulations within the gap-forming regime (see Figure 3) and in other simulations in the literature for the gap-forming regime (Hayasaki et al. 2008; Roedig et al. 2012; Shi et al. 2012).

Regardless of the exact geometry of the density perturbation, in the variety of simulations that examined the interaction of a comparable-mass binary with a gas disk, the torque produced over the binary comes from the same inner region of the disk. For example, in simulations where the density perturbation has an ellipsoidal shape, the exchange of angular momentum between the disk and the binary comes from the gravitational interaction between the binary and the ellipsoidal density perturbation formed in the region of the disk, $r \leqslant 2a$ [as shown in Figure 3(a) and the simulations of Escala et al. 2004, 2005]. In simulations where the binary excavates a gap in the disk, studies have found that the gravitational torque also comes mainly from the inner, $r \leqslant 2a$, region and is associated with the gravitational interaction between the binary and transitory streams of gas falling toward the gap region (Roedig et al. 2012; Shi et al. 2012). This can be seen directly from Figure 5 of Shi et al. (2012) and Figure 9 of Roedig et al. (2012), where they show the surface torque density on the disk associated with the transitory streams of gas. In our simulations, the nonaxisymmetric density perturbation is also formed in the inner region $r \leqslant 2a$. This can be seen in Figure 3, where we show for eight simulations the inner region $r \leqslant 2a$ (white circles).

From our successfully tested gap-opening criterion, we evaluated whether the decrease of the binary separation will lead to the formation of a gap. We find that for a binary embedded in a gas disk with a Mestel density profile (or any steeper density profile), as the binary separation decreases ($a \ll H_{\rm disk}$) the exchange of angular momentum between the binary and the nonaxisymmetric density perturbation will not lead to the formation of a gap. The fast decay of the binary will then continue unless some other process changes the distribution of the gas near the binary.

It is important to note that, in the flat spiral gap-opening criterion [Equation (2)] and the ellipsoidal gap-opening criterion [Equation (1)], the difficulty that a binary has opening a gap in a disk increases with larger values of the dimensionless viscosity parameter $\alpha_{\rm ss}$ of Shakura & Sunyaev (1973). For our SPH simulations, we estimate that $\alpha_{\rm ss} \approx 0.008$–$0.016$ from the value of the SPH parameter for artificial viscosity, $\alpha_{\rm sph}$ (Artymowicz & Lubow 1994; Murray 1996; Lodato & Price 2010; Taylor & Miller 2012). In a massive nuclear disk, the gas will be globally unstable and therefore the torques will be larger, with an $\alpha_{\rm ss}$ of order unity (Krumholz et al. 2007; Escala 2007). Moreover, studies of magnetohydrodynamic (MHD) simulations have found that the presence of MHD stresses can significantly increase the torques, with an effective dimensionless viscosity parameter $\alpha \geqslant 0.2$ (Shi et al. 2012), a factor of $\geqslant$20 greater than the estimated value of $\alpha_{\rm ss}$ in our SPH simulations.

From these estimates, we expect that the value of α_{ss} in real gas-rich astrophysical systems, such as the nuclear disks in ultraluminous infrared galaxies (Downes & Solomon 1998) and submillimeter galaxies (Chapman et al. 2003, 2005; Takoni et al. 2006; Swinbank et al. 2010), will be 1 or 2 orders of magnitude greater than in our simulations. Therefore, in the nuclear regions of gas-rich merging galaxies it is more likely that a SMBH binary will not be able to excavate a gap in the gas, allowing the gravitational torques from the gas to shrink the SMBH binary separation down to scales where gravitational wave emission can drive the final coalescence of the binary.

L.d.V.'s research was supported by CONICYT Chile (grant D-21090518), DAS Universidad de Chile, and Proyecto Anillo de Ciencia y Tecnología ACT 1101. A.E. acknowledges partial support from the Center of Excellence in Astrophysics and Associated Technologies (PFB 06), FONDECYT Regular Grant 1130458. The simulations were performed using the HPC clusters Markarian (FONDECYT 11090216) and Geryon (PFB 06).

REFERENCES

Armitage, P., & Natarajan, P. 2002, ApJL, 567, L9
Armitage, P., & Rice, W. K. M. 2005, in Proc. of the STScI May Symp. 2005: A Decade of Extrasolar Planets Around Normal Stars, Vol. 19, ed. M. Livio et al. (Cambridge: Cambridge Univ. Press), 66
Artymowicz, P., & Lubow, S. H. 1994, ApJ, 421, 651
Artymowicz, P., & Lubow, S. H. 1996, ApJL, 467, L77
Barnes, J., & Hernquist, L. 1992, ARA&A, 30, 705
Barnes, J., & Hernquist, L. 1996, ApJ, 471, 115
Barnes, J. E. 2002, MNRAS, 333, 481
Baruteau, C., & Masset, F. 2013, in Recent Developments in Planet Migration Theory, Tides in Astronomy and Astrophysics, ed. J. Souchay, S. Mathis, & T. Tokieda (Berlin: Springer), 201
Bate, M. R., Lubow, S. H., Ogilvie, G. I., & Miller, K. A. 2003, MNRAS, 341, 213
Boroson, T. A., & Lauer, T. R. 2009, Natur, 458, 53
Bournaud, F., Chapon, D., Teyssier, R., et al. 2011, ApJ, 730, 4
Chapman, S. C., Blain, A. W., Ivison, R. J., & Smail, I. R. 2003, Natur, 422, 695
Chapman, S. C., Blain, A. W., Smail, I. R., & Ivison, R. J. 2005, ApJ, 622, 772
Comerford, J., Gerke, B., Stern, D., et al. 2012, ApJ, 753, 42
Cuadra, J., Armitage, P. J., Alexander, R. D., & Begelman, M. 2009, MNRAS, 393, 1423
del Valle, L., & Escala, A. 2012, ApJ, 761, 31
Dotti, M., Colpi, M., & Haardt, F. 2006, MNRAS, 367, 103
Dotti, M., Sesana, A., & Decarli, R. 2011, AdAst, 2012, 940568
Downes, D., & Solomon, P. M. 1998, ApJ, 507, 615 (DS)
Eracleous, M., Boroson, T. A., Halpern, J. P., & Liu, J. 2011, arXiv:1106.2952
Escala, A. 2007, ApJ, 671, 1264
Escala, A., Larson, R. B., Coppi, P. S., & Mardones, D. 2004, ApJ, 607, 765
Escala, A., Larson, R. B., Coppi, P. S., & Mardones, D. 2005, ApJ, 630, 152
Fabbiano, G., Wang, J., Elvis, M., & Risaliti, G. 2011, Natur, 477, 431
Foreman, G., Volonteri, M., & Dotti, M. 2009, ApJ, 693, 1554
Goldreich, P., & Tremaine, S. 1980, ApJ, 241, 425
Goldreich, P., & Tremaine, S. 1982, ARA&A, 20, 249
Goodman, J., & Tan, J. C. 2004, ApJ, 608, 108
Gultekin, K., Richstone, D. O., Gebhardt, K., et al. 2009, ApJ, 698, 198
Gunther, R., & Kley, W. 2002, A&A, 387, 550
Hayasaki, K., Mineshige, S., & Ho, L. C. 2008, ApJ, 682, 1134
Hayasaki, K., Mineshige, S., & Sudou, H. 2007, PASJ, 59, 427
Hennawi, J. F., Straus, M. A., Oguri, M., et al. 2006, AJ, 131, 1
Hopkins, P. F., & Quataert, E. 2010, MNRAS, 407, 1529
Ivanov, P. B., Papaloizou, J. C. B., & Polnarev, A. G. 1999, MNRAS, 307, 79
Kazantzidis, S., Mayer, L., Colpi, M., et al. 2005, ApJL, 623, L67
Kocsis, B., Haiman, Z., & Loeb, A. 2012a, MNRAS, 427, 2680
Kocsis, B., Haiman, Z., & Loeb, A. 2012b, MNRAS, 427, 2660
Komossa, S., Burwitz, V., Hasinger, G., et al. 2003, ApJL, 582, L15
Komossa, S., Zhou, H., & Lu, H. 2008, ApJ, 678, 81
Krumholz, M., Klein, R., & McKee, C. 2007, ApJ, 656, 959
Levin, Y. 2007, MNRAS, 374, 515
Lin, D. N. C., & Papaloizou, J. 1979, MNRAS, 186, 799
Liu, X., Shen, Y., Strauss, M., & Hao, L. 2011, ApJ, 737, 14
Lodato, G., & Price, D. J. 2010, MNRAS, 405, 1212
MacFadyen, A. I., & Milosavljević, M. 2008, ApJ, 672, 83
Magorrian, J., Tremaine, S., Richstone, D., et al. 1998, AJ, 115, 2285
Mayer, L., Kazantzidis, S., Escala, A., & Callegari, S. 2010, Natur, 466, 1082
Mayer, L., Kazantzidis, S., Madau, P., et al. 2007, Sci, 316, 1874
McKee, C. F., & Ostriker, E. C. 2007, ARA&A, 45, 565
Mestel, L. 1963, MNRAS, 126, 553
Mihos, C., & Hernquist, L. 1996, ApJ, 464, 641
Milosavljević, M., & Phinney, E. S. 2005, ApJL, 622, L93
Miralda-Escude, J., & Kollmeier, J. A. 2005, ApJ, 619, 30
Murray, J. R. 1996, MNRAS, 279, 402
Myers, A. D., Brunner, R. J., Richards, G. T., et al. 2007, ApJ, 658, 99
Myers, A. D., Richards, G. T., Brunner, R. J., et al. 2008, ApJ, 678, 635
Nelson, R. P., & Papaloizou, J. C. 2003, MNRAS, 339, 993
Plummer, H. C. 1911, MNRAS, 71, 460
Richstone, D., Ajhar, E. A., Bender, R., et al. 1998, Natur, 395, 14
Rodriguez, C., Taylor, G. B., Zavala, A. B., et al. 2006, ApJ, 646, 49
Roedig, C., Sesana, A., Dotti, M., et al. 2012, A&A, 545, 127
Sanders, D., & Mirabel, I. 1996, ARA&A, 34, 749
Shakura, N. I., & Sunyaev, R. A. 1973, A&A, 24, 337
Shen, Y., Richards, G. T., Strauss, M. A., et al. 2011, ApJS, 194, 45
Shi, J.-M., Krolik, J. H., Lubow, S. H., & Hawley, J. F. 2012, ApJ, 749, 118
Shu, F. H., Adams, F. C., & Lizano, S. 1987, ARA&A, 25, 23
Springel, V. 2005, MNRAS, 364, 1105
Swinbank, A., Smail, I., Longmore, S., et al. 2010, Natur, 464, 733
Takeuchi, T., Miyama, S. M., & Lin, D. N. C. 1996, ApJ, 460, 832
Takoni, L., Neri, R., Chapman, S., et al. 2006, ApJ, 640, 228
Taylor, P., & Miller, J. 2012, MNRAS, 426, 1687
Tsalmantza, P., Decarli, R., Dotti, M., & Hogg, D. W. 2011, ApJ, 738, 20
Valtonen, M. J., Lehto, H. J., Nilsson, K., et al. 2008, Natur, 452, 851
Ward, W. R. 1997, Icar, 126, 261
Ward, W. R., & Hourigan, K. 1989, ApJ, 347, 490
White, S. D., & Frenk, C. S. 1991, ApJ, 379, 52